Inhibition of voltage-gated sodium ion channel by corannulene and computational inversion blockage underlying mechanisms

Xinyu Li
Nankai University
Hongqiang Yin
Nankai University
Xiang Zuo
Nankai University
Zhenzhen Jia
Nankai University
Yanlei Wang
Chinese Academy of Sciences
Zhuo Yang
Nankai University
Xizeng Feng (xzfeng@nankai.edu.cn)
Nankai University

Research Article

Keywords: Corannulene, Na+ ion channels, Cytotoxicity, Blockage mechanisms

Posted Date: June 17th, 2022

DOI: https://doi.org/10.21203/rs.3.rs-1736491/v1

Abstract

Corannulene (Cor), a special carbon materials, have been evidenced have strong protein binding capacity to regulate lysozyme crystallization and controlling reactive oxygen species (ROS) generation. Ion channel functions are controlled by ion channel protein thus affecting on physiological functions. However, the interaction between Cor and ion channel protein have not been studied. In this study, we used mPEG-DSPE to encapsulate Cor and prepare PEG/Cor complexes. The prepared PEG/Cor complexes distributed in cytoplasm and produced cytotoxicity at high concentration. Whole cell patch clamp examined ion channel functions after PEG/Cor complexes administration. we found that PEG/Cor Nps administration inhibited voltage-gated Na^+ ion channels in a dose-and time-dependent manner but did not act on voltage-gated K^+ ion channels. The potential mechanisms were revealed by all-atom molecular dynamic (MD) simulations. Briefly, Cor could block the pore of sodium ion channel protein due to accumulation of Cor on the pore of ion channel protein. Besides, the orientation angle (θ) configuration of Cor will be inverted with the accumulation to generate two blocking mechanisms. Different from other carbon nanomaterials, the blockage mechanism of Cor provides novel insights into the mechanisms of interaction between carbon nanomaterials and ion channel protein.

Introduction

Carbon-based bio-materials have demonstrated excellent long-term biological performances in biomedicine[1], photothermal therapy[2] and drug delivery[3]. While there exhibited difference biological functions due to their diversity[1]. Corannulene (Cor) is a geodesic polyarene with processes C_{5v} symmetry, which is consisted of a cyclopentane fusing with five benzene rings on the periphery, and exhibiting a bowl-like shape[4–6]. Compared with carbon nanotubes and graphene, Cor has enable da number of unique functions, including binding alkali metal[7], inducing crystalline formation[8], high polymer complexes[4] and others chemical functions[9, 10].Due to these characteristics, Cor is considered as a promising candidate in laboratory research and technological applications. Recently, many efforts have revealed unique functions of Cor on regulating biological processes[4, 5, 8], such as enhancing micelle stability for potential drug carries[11], controlling ROS production[4] and boosting cancer phototheranostics[12].

Cor also displayed special properties on ‘materials-protein’ interaction[6, 8]. Our previous studies showed that Cor processes a far greater binding affinity toward lysozyme than graphene, carbon nanotube and perylene[8]. As a result, the addition of Cor will regulate lysozyme crystallization[8]. Furthermore, Cor has a greater binding capacity to lysozyme than perylene that enhancing its electrostatic interaction with lysozyme[6]. It means that the three-dimensional π-bowl structure and unique charge distribution of Cor will ligate with some binding site of protein thus influencing the biological and catalytic activity of protein[6, 8].Our previous study reported that mPEG encapsulated Cor to prepare PEGlytion/Cor nanoparticles which improved the solubility of Cor and enhanced response stress of mice[5]. However, more detailed and deeper studies need to be done to reveal its biological functions.

It is noteworthy that Cor exhibits extremely poor solubility in water or other biological vehicle, which greatly limits its application[5]. Therefore, various surface coatings were used to functional Cor, such as mPEG-DSPE[4, 5] and cyclodextrin[4]. Poly(ethylene glycol) (PEG) is a coiled polymer of repeating ethylene ether unit with dynamic conformation[9, 13]. PEG is excellently applied in biological researches because characteristics of low toxicity and high biocompatibility[13]. Coating with PEG on the surface of materials or nanoparticles not only improve their solubility, but also increases circulation time versus uncoated counterparts[13]. Above all, functionalizing Cor with PEG improves the solubility of Cor and provides a way to investigate the interaction of organisms.

Carbon nanomaterials have proved various affecting on ion channels behaviors through the “materials-protein” interaction[14–16]. According to the difference topological structure of materials itself, the different interactions of ion channels protein will be generated, so then influencing biological functions[14–16]. For example, K.H. Park suggested that certain diameters SWNTs can efficiently block K^+ channels[15]. A computational study revealed the effects of fullerenes on the functions of K^+ channels[14]. These studies suggested that the topological structure of carbon nanomaterials play an important role in regulating ion channel functions through the interaction between ion channel protein and nanomaterials. Because of the physiological role they play, ion channels are important constituents of the biological system which modulated various intracellular and extracellular process[17], such as neurodegeneration[17] and apoptosis[18]. Therefore, carbon nanomaterials will generate different biological functions in cellular level. However, Cor as a special PAH, with π-bowl structure[4], the relationship between Cor and ion channels have never been reported hitherto. Understanding the interaction between Cor and ion channel will helpful for revealing its biological functions and highlight the “materials-protein” interactions.

In this study, mPEG-DSPE was used to modification Cor through self-assembly non-covalent binding and deliver Cor into PC-12 cell line[5]. We found that PEG/Cor complexes could enter cell and distribute in cytoplasm (Fig. 1a). Then, Whole cell patch clamp was carried out to study the change of ion channels functions after PEG/Cor Nps administration(Fig. 1a). The molecular dynamic was carried out to reveal the interaction between Na^+ channel protein and Cor. The results showed that voltage-gated Na^+ ion channels (Na_Vs)of PC-12 cells were inhibited in time-and dose-dependent by PEG/Cor complexes, but did not occur in pure PEG groups. We speculated there exists two main bio-processes causing the effects. First, Cor-induced production of ROS inhibited activation of voltage-gated Na^+ ion channels. Second, unique topological structure of Cor may blocked the portals of voltage-gated Na^+ ion channels protein. These results demonstrated that the Cor has the potential to inhibit activation of Na_Vs as a Na + ion channels blocker and highlight a novel mechanism for “materials-protein” interaction

Results And Dissusion

Characterization of PEG/Cor Nps

Cor exhibits poor solubility in a various physiological vehicle which limits the applications in organisms[5]. Thus, mPEG-DSPE was used to prepare PEG/Cor Nps by an emulsified evaporation method. The PEG/Cor Nps exhibited better dispersibility than bulk Cor which has been evidenced in our previous study[5]. Cor exhibited blue fluorescence, larger flake or lump shape with more than 200 μm sizes under 270 nm excitation wavelength **(**Fig. 1b**)**. However, PEG/Cor Nps presented tiny particles with blue fluorescence**(**Fig. 1b**)**. Transmission electron microscope (TEM) and atomic force microscope (AFM) were carried out to observe the PEG/Cor Nps after vacuum drying and re-dissolution. The PEG/Cor Nps presented spherical nanoparticles with 30–50 nm size**(**Fig. 1c, d**)**. These results suggested that the size of PEG/Cor Nps to be in the nanometer range with auto purple fluorescence. Particle size is an important parameter in designing suitable cell tracking and drug carries system because it determines the rate of cell uptake[19]. F. Lu *et.al.* suggested that the maximum rate of cells uptake occurred at nanoparticles of 50 nm[19]. It means that the PEG/Cor Nps have a good rate of cell uptake that is an essential element in nano-scale drug carries and cell imaging[19].Comparing with other organic-nanoparticles, such as fullerene nanoparticles which the size range is 110–340 nm[20], the prepared PEG/Cor Nps exhibited smaller size. Thus, Cor could provide a kind of 3D structure PAH skeleton for preparing smaller organic nanoparticles than fullerene and carbon tube.

In vitro toxicity of PEG/Cor Nps to PC-12 cells

PC-12 cells were co-cultured with PEG/Cor Nps for 4h and observed under confocal microscopic images after removing redundant PEG/Cor Nps. The results showed PEG/Cor Nps distributed in the cytoplasm but did not penetrate the nucleus **(Fig. 2a, c)**.Comparing with previous studies, PEG/Cor Nps have stronger auto-fluorescence intensity than FITC-labeled mesoporous silica nanoparticles[19] and Texas Red-labeled fullerenes nanoparticles[21]. It means that the Cor have potential values in cell imaging and photodynamic therapy**(Fig. 2c)**[4, 12, 22]. S. Liu *et.al.* supported that the Cor preferred mitochondria accumulation due to the large negative membrane potential of mitochondria. In this study, however, we did not co-locate Cor with mitochondria[22].

The viability of PC-12 cells was determined by the standard cytotoxicity test. The viability and inhibiting rate were presented time-dependent and dose-dependent manners after PEG/Cor Nps treatment. The half maximal inhibitory concentration (IC_{50}) was calculated as 10 μg/mL (72h co-culture), 20 μg/mL (50h co-culture), 40 μg/mL (4h co-culture) and 50 μg/mL (3h co-culture) **(Fig. 2b)**. It means that the cytotoxicity of PEG/Cor Nps dependent on adding concentration and culturing time. Regarding 5 μg/mL, cell viability did not show half maximal inhibitory rate after 72h co-culture **(Fig. 2b)**. L. Zhang and S. Liu reported that Cor has functioned in controlling ROS production[22]. According to this study, Cor could induce a higher extent of cytotoxicity and thus more satisfactory therapeutic outcomes than perylene[22]. Nevertheless, our results showed that PEG/Cor Nps have characteristics of low cytotoxicity, high rate of cell uptake and fluorescence intensity at 5μg/ml concentration. Therefore, we speculated that Cor-based nanoparticles have potential values in cell imaging and drug carries at low concentration.

The dose-dependent effects of PEG/Cor Nps on whole-cell ion currents

Carbon nanomaterials have been evidenced to have impacts on regulating ion channels[15, 16]. For example, SWCNTs can physically occlude the potassium voltage-gated channel[15] and inhibit calcium ion channel activation through releasing yttrium[16]. Carbon materials were therefore used to regulate physical functions and cell behaviors, such as calcium-dependent cellular functions of growing neurons [23] and cell death controlling[16]. A highlight study demonstrated the pore occlusion mechanism and suggested the diversity of the topological structure of carbon materials can induce different ion channel behaviors[15]. Cor as novel carbon nanomaterials, the effects on ion channel behaviors was examined by whole cell patch clamp.

According to our present study, PEG/Cor Nps concentration at 5μg/mL was selected to investigate the behaviors of ion channels. All test cells were held at -60 mV and the current traces were evoked by using 300 ms constant depolarizing pulse from − 50 mV to + 90 mV in increments of 10 mV during the recording of whole-cell ion currents. The inward currents and outward currents of the registered cells showed typical voltage-gated Na^+ currents and K^+ currents. Electrophysiological behavior is similar to what was reported in other studies**(Fig. 3a)**[24]. The activated inward current could be completely blocked by bath application of 0.5 mM TTX **(Fig. 3a)**, indicating that voltage-gated sodium current carries the largest inward currents. The application of PEG/Cor Nps in different dose produced obvious inhibiting effects on inward currents (voltage-gated Na^+ currents) **(Fig. 3a, c)** but no significant changes on outward currents (voltage-gated K^+ currents) **(Fig. 3b, e)**. The activation curves of inward currents produced depolarization shifts with the increasing of PEG/Cor Nps**(Fig. 3d)**. It means that PEG/Cor Nps reduce the opening number of voltage-gated Na^+ currents at each command potential in PC-12 cells as the dose increased[25]. These results suggested the PEG/Cor Nps have dose-dependent effects on inhibiting voltage-gated Na^+ currents activation.

The time-dependent effects of PEG/Cor Nps on whole-cell ion currents

Previous studies demonstrated Cor-based systems could generate ROS in dose- and irradiation time-dependent manner[4]. Moreover, our present study revealed the cytotoxicity of PEG/Cor complexes were related on co-culturing time. We speculated the inhibition of PEG/Cor Nps to ion channel behaviors exists time-dependent manners. The dose of PEG/Cor Nps at 1μL which exhibited no significant influence on voltage-gated sodium channels after 1 min co-cultured, was used to examine the time-dependent effects. Experiments were performed at 1, 5, and 10 min respectively after PEG/Cor Nps treated to PC-12 cells. The results showed that the inward currents of PC-12 cells were inhibited after 5 min co-culturing with PEG/Cor complexes **(**Fig. 4a, b **and c)**. Compared amplitude of inward currents of 5 min and 10 min, the effect of inhibition was increased with the increasing of culture time **(**Fig. 4c**)**. From Fig. 4d, the activation curves of inward currents also showed depolarization shifts as time increased **(**Fig. 4d**)**.. These results

suggested that the PEG/Cor Nps have time-dependent effects on inhibiting voltage-gated sodium channels.

mPEG-DSPE did not alter whole-cell ion currents

In order to determine whether mPEG-DSPE has effects on whole-cell ion currents, we also detected the effect of mPEG-DSPE on whole-cell ion currents in PC-12 cells. In the preparation process of PEG/Cor Nps, mPEG-DSPE and Cor were 4:1 mixed. Thus, the amount of mPEG-DSPE was calculated then concentrated to 20μg/mL. We added 6μL mPEG-DSPE aqueous to culture with PC-12 cells. Because of adding 6μL PEG/Cor Nps inhibited inward currents. We found that adding 6μL mPEG-DSPE aqueous did not alter inward and outward current after co-cultured 5 min and 10 min **(Supplementary Fig. 1a, b and c)**. The amplitude of inward and outward currents also did not change than the control group **(Supplementary Fig. 1a, b and c)**. These results demonstrated the mPEG-DSPE cannot induce the change in inward currents. Thus, we speculated that the inhibition of voltage-gated sodium channels due to the released Cor form PEG/Cor Nps in the cytoplasm.

Molecular dynamics (MD) simulations for pore occlusion mechanism

All-atom molecular dynamics (MD) simulations were carried out to capture the undying mechanism of Cor molecule blocking the sodium channel[26–28]. As shown in **Fig. 5a**, we construct a cell membrane embedding a sodium protein in the center, while two sides are covers by enough water molecules representing the real environment in the life system. The number of Cor (*N*) molecules will be placed in the inner side of the cell membrane (**Fig. 5b**) considering that the Cor will be delivered into the cell directly as the experimental results shown that. To measure the structure change of protein induced by the Cor, we calculate the Root-Mean-Square Deviation (RMSD) via the flowing equation[29],

$$\mathrm{RMSD}=\left\langle \sqrt{\frac{1}{M}\sum_{i=1,M}\delta_i^2} \right\rangle \quad (3)$$

Where M is the total number of atoms, δ_i is the distance between the i^{th} atom and the reference structure, the angular bracket representing the average of the total simulation time. As shown in **Fig. 5c**, the RMSD will increase firstly and then up to the convergence stage at about 1 ns. The average of RMSD in the last 1 ns was summarized to quantificationally describe the influence of Cor on the protein **(Fig. 5d)**. The fact can be concluded that the influence will be larger when more Cor molecules accumulated in the system, which will introduce a significant effect on blocking the pore of sodium protein.

We further summarized the configurations of Corto describe the mechanism of Cor molecule blocking the protein channel. From the results, the Cor will accumulate near the pore of the channel protein at lower concentration (N = 8) to block the pore of the channel protein **(Fig. 6a, b)**. As the time increases, the concentration of Cor will be increased and prefer aggregate to a cluster near the inner surface of the

protein (**Fig. 6c, d)** (*N* = 80). Both cases would block the protein channel and inhibit sodium ion channel functions, which agrees well with the above experimental results. These two different mechanisms can be explained well via the analysis of energy. First, the small molecules prefer to aggregate in the water environment, upping to the lowest total energy. So, Cor will form a cluster at higher concentration (**Fig. 6c, d)**. However, at lower concentration, the interfacial energy between Cor and protein will be larger than the interfacial energy within the Cor, and then Cor will be absorbed onto the surface of the protein and even enter the channel of protein. Besides, the result also explains the time-dependent manner of blocking effects. As the time increasing, Cor will be absorbed by the protein and increases concentration of Cor while causing inhibition from low to high concentration stage.

Moreover, we found that the effects of Cor on blocking sodium ion channel function dependents on the orientation angle (θ) configuration of Cor in the system, which is defined as the included angle between the *z*-direction and the normal direction of Cor (**Fig. 7a**). For the first, the orientation angle has an almost uniform distribution ranging from 0° to 180° for different concentration of Cor. The time evolution of the orientation angle is very important for the configuration of Cor in the system and the blocking mechanism of protein. The orientation angle as a function of time is summarized, implying that the change of angle depends greatly on the concentration **(Fig. 7b)**. At low concentration (N = 8), the orientation angle can change greatly between “rim-to-protein” and “bottom-to-protein” states. As the time increase, Cor will be enriched leading to increase of concentration, the orientation angle will have small variation and maintain the initial state.

In present study, we demonstrated PEG/Cor complexes could accumulate in cytoplasm of PC-12 cells. It is important that the accumulated PEG/Cor complexes could dose-dependent and time-dependent inhibit voltage-gated Na^+ currents but pure mPEG-DSPE did not have this function. Thus we speculated voltage-gated Na^+ currents were inhibited as a result of releasing and accumulating of Cor. Many of the most common diseases involve abnormalities of voltage-gated Na^+ currents, such as cancer[18], neurological disorder[17, 30] and cardiovascular diseases[27, 31]. These functions of voltage-gated Na^+ currents make it easy targets for external agents such as natural toxins and synthetic drugs that react with them by establishment electrochemical interactions[15, 28]. Therefore, these findings postulate new uses for Cor in biological applications.

The mechanisms of Cor inhibiting voltage-gated Na^+ currents were discussed according to previous studies. First, the voltage-gated Na^+ currents were reduced during oxidative stress[32]. Eliminating ROS could decrease the response of inhibiting voltage-gated Na^+ currents[33]. Curved Cor induced dipole moment aids electron transfer and enhance enables ROS generation[4, 22]. These studies suggested the Cor-induced production of ROS play a key role in inhibiting voltage-gated Na^+ currents**(**Fig. 8b**)**. Moreover, topological structure of carbon materials may influenced the response of ion channels[15]. K. H. Park *et.al.* made a study which compared the ion channels functions of PC-12 cells after treatment with SWCNTs, MWCNTs and fullerenes[15]. They suggested that the carbon materials have effects on blocking K^+ channels and the blockage was dependent on the shape and dimension of materials

used[15]. Cor as a bowl-shape three dimension carbon materials, may inhibited voltage-gated Na^+ currents by blocking the pore of sodium ion channel protein as similar as SWCNTs[15]. However, this effects were decided by the sodium ion channel protein subunit induced pore regulating mechanisms[34]. For example, *Arcobacterbutzleri* voltage-gated Na^+ channel protein (Na_VAb)with an orifice of ~ 4.6×4.6 Å moved only ~ 1 Å**(**Fig. 8a **red)**[30, 34, 35]. Therefore, the Cor (~ 7.2 Å) cannot passed the pore and blocked on it, such as pore-blocking toxin tetrodotoxin[30]. Regarding *Magnetococcussp* voltage-gated Na^+ channel protein (Na_VMs), the pore S6 segments displaced at ~ 2.5 Å scale, would result in an aperture in the activation gate with a diameter > 8 Å**(**Fig. 8a **blue)**[34].The aperture was easily sufficient for Cor to pass through. These general pore architecture reveals the structural basis for gated access of blocking ions and drugs to the lumen of the pore observed in classical studies of ion selective and pore block[15, 34, 35]. This mechanism appears to be governed by geometrical factors as a “physical barrier” [15]and lacks any other biological/chemical component that usually required by conventional agents[36]. However, the specific experiment and molecular simulation needs to be studied in the future to reveal the really mechanisms[14, 16].

Conclusion

In summary, the current work highlights the importance of PEG/Cor Nps in realizing inhibited voltage-gated Na^+ currents. However, voltage-gated Na^+ currents did not change after pure mPEG-DSPE treatment. We therefore speculated that bulk Cor have effects on inhibiting voltage-gated Na^+ currents. The interaction between sodium ion channel protein and Cor was calculated by MD to reveal the pore occlusion mechanism of Cor. Interestingly, the blocking effects of Cor on sodium ion channel protein dependent on the concertation of Cor accumulation. Thus, Cor have potential values on regulating ion channel functions. However, how to control the direction of Cor will be a challenge. In present study, our results open the novel avenues of bio-electrophysiology application of Cor.

Experimental Section

Preparation of PEG/Cor Nps

1,2-distearoyl-sn-glycero-3-phosphoethanolamine-N-[amino(polyethyleneglycol)-2000] ($mPEG\text{-}DSPE_{2000}$) were purchased from Tebu-Bio company (Catalog number: PG-1-DS-2K). Cor was synthesized and provided by J. S. Siegel’s laboratory. Preparation of PEG/Cor Nps followed our previously described methods[5]. In brief, 1 mg Cor and 4 mg mPEG-DSPE dissolved in 500 µL of tetrahydrofuran (THF) and distilled water at 78^oC, respectively. Then, these two dissolutions were cautiously added to 10mL distilled water with ultrasonic emulsification (1.5s/2s) for 1h. The mixed solution was transferred to a water bath under 60^oC for 24h to eliminate THF. After vacuum freeze-drying, adding 1mL distilled water concentrated to 1 mg/mL and stored in 4^oC.

PC-12 Cells culture

PC-12 cells were cultured in DMEM supplemented with 10% FBS, 1% penicillin, and 1% streptomycin in a humidified 5% CO_2 incubator at 37^oC. The culture medium was changed every other day. After PC-12 cells hovering around 80% confluence, they were plated onto glass coverslips coated with poly-D-lysine/laminin in the six-well tissue culture plates and cultured with DMEM containing 2% FBS, 1% penicillin, and 1% streptomycin with NGF (nerve growth factor, 50 ng/ml) three days. The differentiated cells attached on coverslips were employed for the study of whole-cell patch-clamp recording.

Cell viability assay

Cell viability assay was based on the tetrazolium salt 3-[4,5-dimethylthiazol-2-yl]-2,5- diphenyltetrazolium bromide (MTT). PC-12 cells were divided into six groups: (1) Black control group; (2) PC-12 cells treated with 5 μg/mL, 10 μg/mL, 20 μg/mL, 40 μg/mL and 50 μg/mL PEG/Cor Nps, respectively. Before MTT assay, PC-12 cells were cultured in 96-plates (1×10^4 cells/wall) to reached approximately 70% confluence. Each group had five repetitions. Then, PEG/Cor Nps in different concentrations were added in PC-12 cells of 96-plates, and the cells were incubated at 37^oC for 4 h, 24 h, 48 h and 72 h, respectively. MTT solution (10 μL, 5mg/mL) was added into plates and co-treatment at 37^oC for 4 h. Next, mediums were removed and 100 μL DMSO was added to dissolve the formazan. The optical density value was detected by a microplate reader at 595 nm. The MTT values were used to analyze the cytotoxicity of PEG-Corannulene nanoparticles.

Whole-cell patch-clamp recording

The conventional whole-cell patch-clamp recording was carried out at room temperature (25^oC). The differentiated PC-12 cells attached on glass coverslips were performed and the coverslips were transferred immediately to a recording chamber on a stage of Olympus inverted microscope (BX51WI, Olympus, Japan) before recording. The extracellular or bath solution intracellular solution contained (in mM): NaCl 125, $NaHCO_3$ 25, NaH_2PO_4 1.25, D-glucose 10, KCl 1.25, $CaCl_2$ 2.0, $MgCl_2$ 2.0, adjusted to pH 7.4 with NaOH. The standard pipette solution contained (in mM): KCl 140, $MgCl_2$ 2, HEPES 10, EGTA 10, ATP-Na_2 2, buffered to pH 7.4 with KOH. The cells were visualized on a television monitor connected to a low light sensitive CCD camera (710M, DVC, USA). The path electrodes made of borosilicate glass had an electrical resistance of 3–8 MΩ pulled by a multistage micropipette puller (P-97, Sutter Instruments, USA). After formation of whole-cell clamp configuration, the cells were stabilized for 5min before starting the pulse protocols and the currents were recorded as a control group. Then each concentration of PEG/Cor Nps was administered to the cells respectively to detect the effect on the whole-cell ion currents. Moreover, the whole-cell ion currents of each time point (1min, 5min, 10min) were also detected at a certain concentration. During the recording, all the signals were low-pass filtered at 3kHz and digitized at 10kHz. And the cells were chosen only when the seal resistance was greater than 500 MΩ and the series resistance was less than 30 MΩ. Only one cell on the coverslips was used for any given experiment. Tetrodotoxin (TTX) was used to examine the voltage-gated sodium currents carries the largest inward currents. TTX was purchased from the Research Institute of the Aquatic Products of Hebei (China).

Atomic structures.

We construct the cell membrane by embedding a sodium channel protein (Na_vAb, PDB code:5vb8) in hydrated palmitoyl oleyl phosphatidyl choline (POPC) lipid bilayer at the center region. Two sides of the cell membrane are immersed in water representing a relative practical cell environment. Then we randomly placed several corannulenes in the inner side of the cell membrane. Such a system is consisting of 173 POPC lipid molecules, 1 channel protein, 6130 water molecules in the inner side, 5652 water molecules in the outer side, and several corannulenes (*N*). Besides, 4 Cl- is added to ensure electroneutrality of the system. A two-dimensional supercell is used with periodic boundary conditions along the cell membrane, with lateral dimensions of 10.10 and 10.01 nm, and an open boundary condition is used in the direction across the cell membrane. This model has been successfully used to predict the structural and thermal behavior of lipid bilayer[29, 37].

Molecular dynamics (MD) simulations.

All classical MD simulations are completed using the large-scale atomic/molecular massively parallel simulator package (LAMMPS)[38]. The thermodynamics, structural and mechanical properties of lipid bilayers and proteins in the cell membrane have been successfully explored using this approach[14, 37, 39]. However, the salt and pH effects are not considered in the current model because of the low concentrations of ions and limited system size in all-atomic simulations. The CHARMM36 force field is used for the protein and lipid bilayer, and the TIP3P model is used for water. The interatomic interactions for corannulene are representing using the all-atom optimized potential for liquid simulations (OPLS)[40]. The interaction between water, corannulene, lipid bilayer, and protein include both van der Waals and electrostatic terms. The former one, van der Waals, is described by the 12 − 6 Lennard-Jones potential and truncated at 1.2 nm, while the long-range Coulomb interactions are computed using the particle-particle-particle-mesh algorithm[39]. The timestep is set to 0.5 fs to assure energy conservation in the absence of thermostat coupling. The whole system is equilibrated at 300 K and 1 atm using NPT ensemble.

Data analysis

Data were obtained from patch clamp amplifier (HEKA, EPC 10, Germany). And the data was analyzed by using Clamp fit 9.0, Origin 7.5 and SPSS 11.5. The data were presented as mean ± S.E.M. Statistical significance was assessed using a Student's paired or unpaired t-test when there were only two groups involved. The significant level was set at $p < 0.05$. For the analysis of the steady-state kinetics of currents, the amplitudes of currents at each test potential were converted to conductance (G) by the formula:

$$G = I/(V-V_k)$$

where V_k is the reverse potential. The conductance at each command potential was normalized to G_{max}. Then the normalized value of G/G_{max} was plotted against the test potential to produce voltage-conductance relationship curves, which were fitted by the Boltzmann function:

$$G/G_{max}=1//\{1 + \exp[-(V-V_h)/k]\}$$[28]

where V_h is the potential at half-maximal conductance and k is slope factor.

Declarations

Supporting Information

Supporting Information is available from the Wiley Online Library or from the author.

Acknowledgements

Not applicable.

Author contributions

X.Z.F. and X.Y.L. designed the experiments. X.Y.L and Z.Z.J. performed cell experiments including PC-12 cell imaging and MTT assess; H.Q.Y. and Z.Y carries the whole cell patch clamp examine. Y.L.W calculate interaction between protein and Cor. X.Y.L, organized whole experiments. X.Y.L, Y.L.W, H.Q.Y and X.Z. draft this manuscript.

Funding

We thank the National Basic Research Program of China (2015CB856500), Youth Innovation Promotion Association CAS (2021046) and Special Fund for Basic Research on Scientific Instruments of the Chinese National Natural Science Foundation (Grant no: 62027812) for support of this work.

Availability of data and materials

The datasets and materials used in the study are available from the corresponding author.

Ethics approval and consent to participate

Not applicable.

Consent for publication

Not applicable.

Competing interests

The authors declare no competing financial interest.

Author details

a. State Key Laboratory of Medicinal Chemical Biology, Key Laboratory of Bioactive Materials, Ministry of Education, College of Life Sciences, Nankai University, Tianjin 300071, China.
b. College of Medicine, State Key Laboratory of Medicinal Chemical Biology, Key Laboratory of Bioactive Materials Ministry of Education, Nankai University, Tianjin 300071, China.
c. Beijing Key Laboratory of Ionic Liquids Clean Process, CAS Key Laboratory of Green Process and Engineering, Institute of Process Engineering, Chinese Academy of Sciences, Beijing 100190, P. R. China.

References

1. Xue X, Yang JY, He Y, Wang LR, Liu P, Yu LS, Bi GH, Zhu MM, Liu YY, Xiang RW, et al: **Aggregated single-walled carbon nanotubes attenuate the behavioural and neurochemical effects of methamphetamine in mice.** *Nat Nanotechnol* 2016, **11**:613–620.
2. Yang K, Wan J, Zhang S, Tian B, Zhang Y, Liu Z: **The influence of surface chemistry and size of nanoscale graphene oxide on photothermal therapy of cancer using ultra-low laser power.** *Biomaterials* 2012, **33**:2206–2214.
3. Wang R, Cherukuri P, Duque JG, Leeuw TK, Lackey MK, Moran CH, Moore VC, Conyers JL, Smalley RE, Schmidt HK, et al: **SWCNT PEG-eggs: Single-walled carbon nanotubes in biocompatible shell-crosslinked micelles.** *Carbon* 2007, **45**:2388–2393.
4. Zhang L, Dong X, Lu D, Liu S, Ding D, Kong D, Fan A, Wang Z, Zhao Y: **Controlled ROS production by corannulene: the vehicle makes a difference.** *Biomater Sci* 2017, **5**:1236–1240.
5. Li X, Sun D, Li X, Zhu D, Jia Z, Jiao J, Wang K, Kong D, Zhao X, Xu L, et al: **PEGylation corannulene enhances response of stress through promoting neurogenesis.** *Biomater Sci* 2017, **5**:849–859.
6. Du S, Wang H, Yang Y, Feng X, Shao X, Chipot C, Cai W: **Curvature of Buckybowl Corannulene Enhances Its Binding to Proteins.** *The Journal of Physical Chemistry C* 2018, **123**:922–930.
7. Wu D, Shao T, Men J, Chen X, Gao G: **Superaromatic terpyridines based on corannulene responsive to metal ions.** *Dalton Trans* 2014, **43**:1753–1761.
8. Li X, Wang H, Kuang X, Ma J, Feng X: **Exploring the effects and mechanisms of carbon nanomaterial diversity on the morphology of lysozyme crystals.** *CrystEngComm* 2017, **19**:5873–5881.
9. Juricek M, Strutt NL, Barnes JC, Butterfield AM, Dale EJ, Baldridge KK, Stoddart JF, Siegel JS: **Induced-fit catalysis of corannulene bowl-to-bowl inversion.** *Nat Chem* 2014, **6**:222–228.
10. Yilmaz B, Bjorgaard J, Colbert CL, Siegel JS, Kose ME: **Effective solubilization of single-walled carbon nanotubes in THF using PEGylated corannulene dispersant.** *ACS Appl Mater Interfaces* 2013, **5**:3500–3503.
11. Dong X, Guo X, Liu G, Fan A, Wang Z, Zhao Y: **When self-assembly meets topology: an enhanced micelle stability.** *Chem Commun (Camb)* 2017, **53**:3822–3825.
12. Gu X, Zhang X, Ma H, Jia S, Zhang P, Zhao Y, Liu Q, Wang J, Zheng X, Lam JWY, et al: **Corannulene-Incorporated AIE Nanodots with Highly Suppressed Nonradiative Decay for Boosted Cancer**

Phototheranostics In Vivo. *Adv Mater* 2018, **30**:e1801065.

13. Jokerst JV, Lobovkina T, Zare RN, Gambhir SS: **Nanoparticle PEGylation for imaging and therapy.** *Nanomedicine (Lond)* 2011, **6**:715–728.
14. Kraszewski S, Tarek M, Treptow W, Ramseyer C: **Affinity of C60 neat fullerenes with membrane proteins: a computational study on potassium channels.** *ACS Nano* 2010, **4**:4158–4164.
15. Park KH, Chhowalla M, Iqbal Z, Sesti F: **Single-walled carbon nanotubes are a new class of ion channel blockers.** *J Biol Chem* 2003, **278**:50212–50216.
16. Jakubek LM, Marangoudakis S, Raingo J, Liu X, Lipscombe D, Hurt RH: **The inhibition of neuronal calcium ion channels by trace levels of yttrium released from carbon nanotubes.** *Biomaterials* 2009, **30**:6351–6357.
17. Kumar P, Kumar D, Jha SK, Jha NK, Ambasta RK: **Ion Channels in Neurological Disorders.** *Adv Protein Chem Struct Biol* 2016, **103**:97–136.
18. Lastraioli E, Iorio J, Arcangeli A: **Ion channel expression as promising cancer biomarker.** *Biochim Biophys Acta* 2015, **1848**:2685–2702.
19. Lu F, Wu SH, Hung Y, Mou CY: **Size effect on cell uptake in well-suspended, uniform mesoporous silica nanoparticles.** *Small* 2009, **5**:1408–1413.
20. Sugikawa K, Kozawa K, Ueda M, Ikeda A: **Size controlled fullerene nanoparticles prepared by guest exchange of γ-cyclodextrin complexes in water.** *RSC Advances* 2016, **6**:74696–74699.
21. Dellinger A, Zhou Z, Norton SK, Lenk R, Conrad D, Kepley CL: **Uptake and distribution of fullerenes in human mast cells.** *Nanomedicine* 2010, **6**:575–582.
22. Liu S, Lu D, Wang X, Ding D, Kong D, Wang Z, Zhao Y: **Topology dictates function: controlled ROS production and mitochondria accumulation via curved carbon materials.** *J Mater Chem B* 2017, **5**:4918–4925.
23. Ni Y, Hu H, Malarkey EB, Zhao B, Montana V, Haddon RC, Parpura V: **Chemically functionalized water soluble single-walled carbon nanotubes modulate neurite outgrowth.** *J Nanosci Nanotechnol* 2005, **5**:1707–1712.
24. Morales-Reyes I, Seseña-Rubfiaro A, Acosta-García MC, Batina N, Godínez-Fernández R: **Simultaneous recording of the action potential and its whole-cell associated ion current on NG108-15 cells cultured over a MWCNT electrode.** *Measurement Science and Technology* 2016, **27**.
25. Toma T, Logan MM, Menard F, Devlin AS, Du Bois J: **Inhibition of Sodium Ion Channel Function with Truncated Forms of Batrachotoxin.** *ACS Chem Neurosci* 2016, **7**:1463–1468.
26. Catterall WA: **Voltage-Gated Sodium Channels: Structure, Function, and Pathophysiology.** In *Encyclopedia of Biological Chemistry.* 2013: 564–569
27. Dahlberg J, Sjogren M, Hedblad B, Engstrom G, Melander O: **Genetic variation in NEDD4L, an epithelial sodium channel regulator, is associated with cardiovascular disease and cardiovascular death.** *J Hypertens* 2014, **32**:294–299.

28. Keefer EW, Botterman BR, Romero MI, Rossi AF, Gross GW: **Carbon nanotube coating improves neuronal recordings.** *Nat Nanotechnol* 2008, **3**:434–439.
29. Coutsias EA, Seok C, Dill KA: **Using quaternions to calculate RMSD.** *J Comput Chem* 2004, **25**:1849–1857.
30. Catterall WA: **Voltage-gated sodium channels at 60: structure, function and pathophysiology.** *J Physiol* 2012, **590**:2577–2589.
31. ten Eick RE, Whalley DW, Rasmussen HH: **Connections: heart disease, cellular electrophysiology, and ion channels.** *Faseb j* 1992, **6**:2568–2580.
32. Barrington PL, Martin RL, Zhang K: **Slowly inactivating sodium currents are reduced by exposure to oxidative stress.** *J Mol Cell Cardiol* 1997, **29**:3251–3265.
33. Liu Z, Liu S, Ren G, Zhang T, Yang Z: **Nano-CuO inhibited voltage-gated sodium current of hippocampal CA1 neurons via reactive oxygen species but independent from G-proteins pathway.** *J Appl Toxicol* 2011, **31**:439–445.
34. McCusker EC, Bagneris C, Naylor CE, Cole AR, D'Avanzo N, Nichols CG, Wallace BA: **Structure of a bacterial voltage-gated sodium channel pore reveals mechanisms of opening and closing.** *Nat Commun* 2012, **3**:1102.
35. Payandeh J, Scheuer T, Zheng N, Catterall WA: **The crystal structure of a voltage-gated sodium channel.** *Nature* 2011, **475**:353–358.
36. Zhang MM, Wilson MJ, Azam L, Gajewiak J, Rivier JE, Bulaj G, Olivera BM, Yoshikami D: **Co-expression of Na(V)beta subunits alters the kinetics of inhibition of voltage-gated sodium channels by pore-blocking mu-conotoxins.** *Br J Pharmacol* 2013, **168**:1597–1610.
37. Wang Y, Qin Z, Buehler MJ, Xu Z: **Intercalated water layers promote thermal dissipation at bio-nano interfaces.** *Nat Commun* 2016, **7**:12854.
38. Plimpton S: **Fast parallel algorithms for short-range molecular dynamics.** *Journal of computational physics* 1995, **117**:1–19.
39. Song Z, Wang Y, Xu Z: **Mechanical responses of the bio-nano interface: A molecular dynamics study of graphene-coated lipid membrane.** *Theoretical and Applied Mechanics Letters* 2015, **5**:231–235.
40. Jorgensen WL, Maxwell DS, Tirado-Rives J: **Development and testing of the OPLS all-atom force field on conformational energetics and properties of organic liquids.** *Journal of the American Chemical Society* 1996, **118**:11225–11236.

Figures

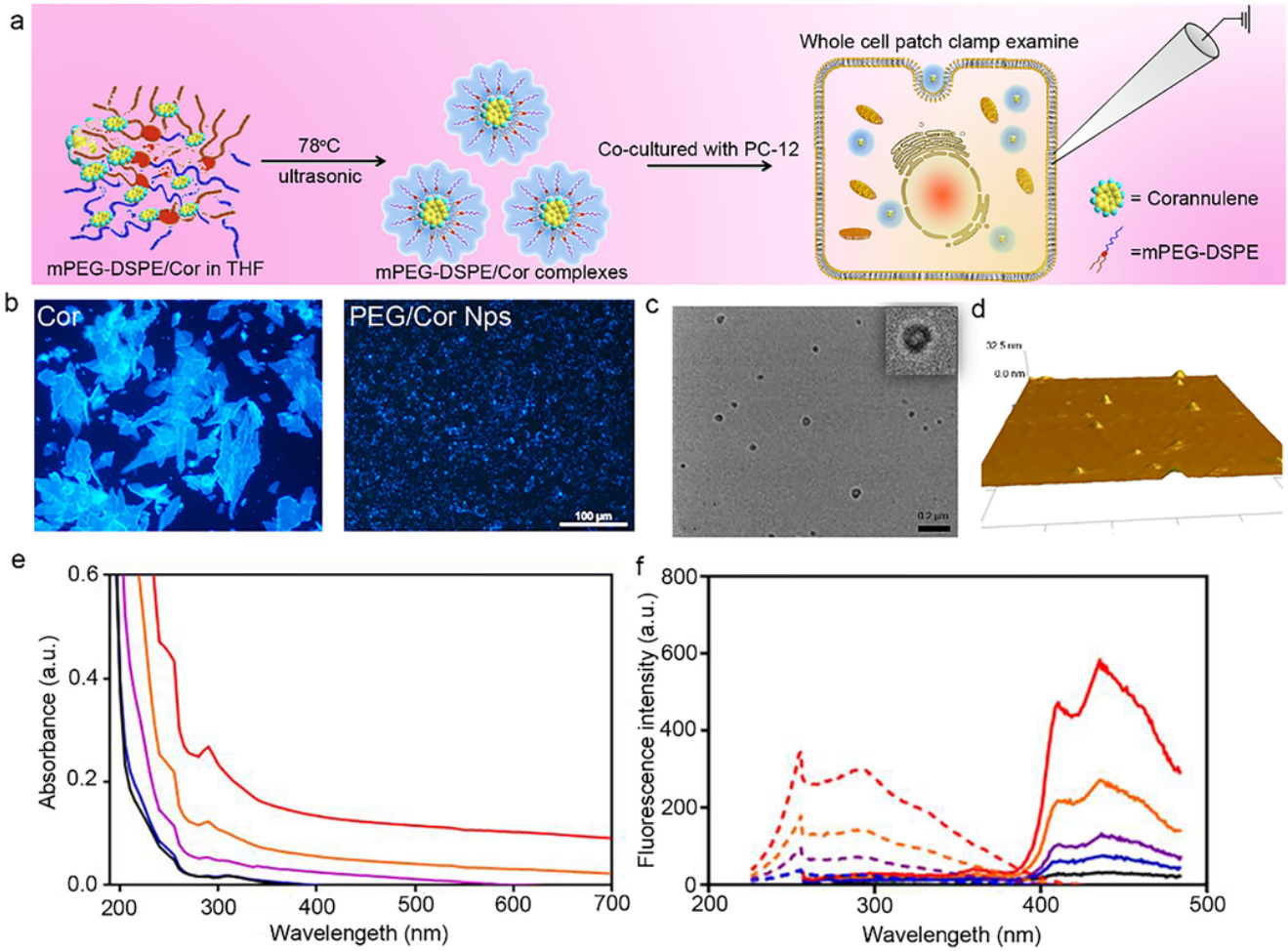

Figure 1

Scheme of experimental process and characteristics of PEG/Cor Nps. (a) Scheme of the experimental process. mPEG-DSPE/water solution and Cor/THF solution were mixed in ultrapure water under 78°C with ultrasonic emulsification. The PEG/Cor Nps were co-cultured with PC-12 cells to examine the activation of ion channels. (b) Photos of Cor and PEG/Cor Nps under UV light. (c) TEM imaging of PEG/Cor Nps. (d) Three-dimensional AMF imaging of PEG/Cor Nps. (e) The absorption spectrum of PEG/Cor Nps. (f) Emission spectrum and excitation spectrum of PEG/Cor Nps.

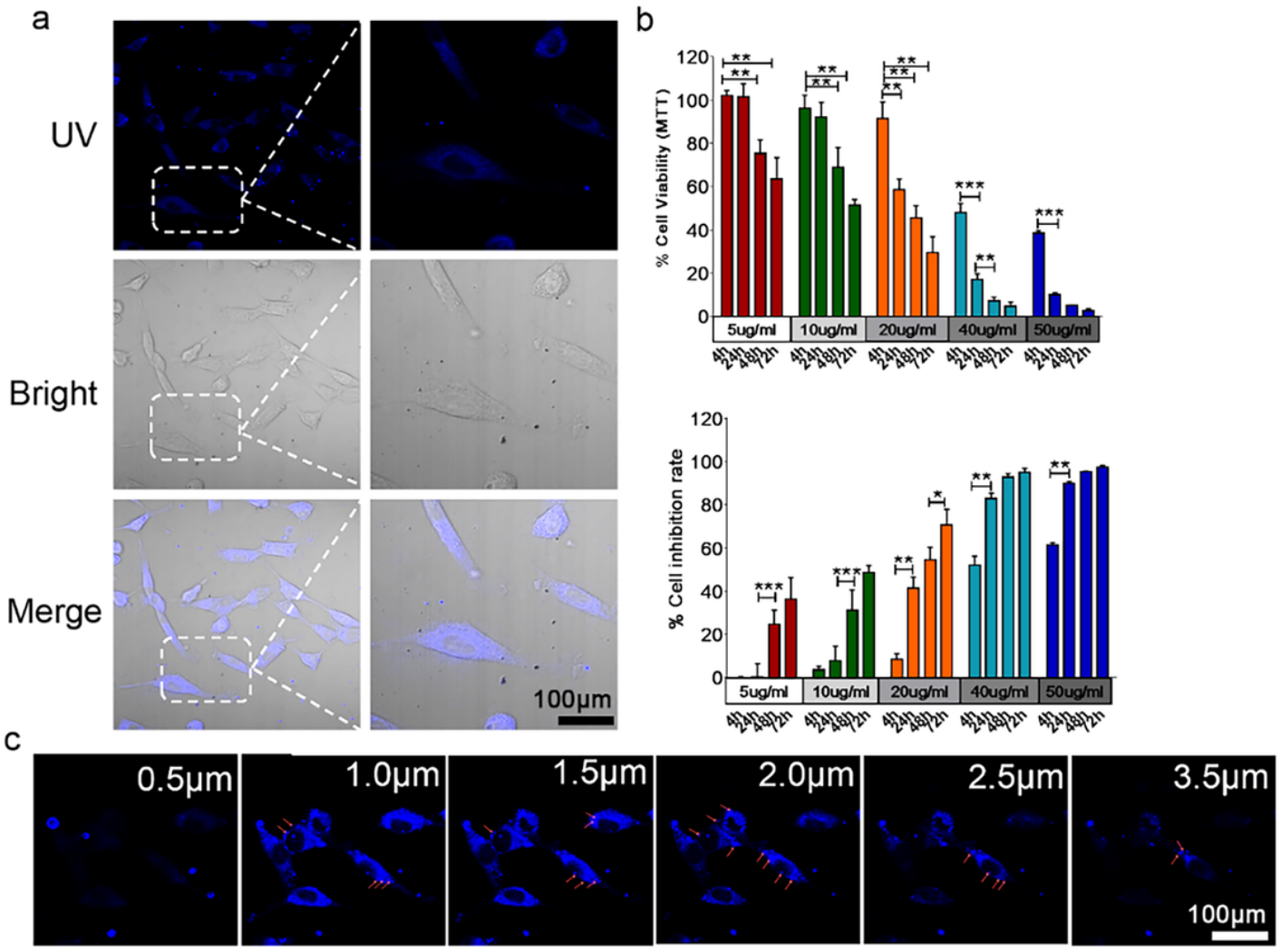

Figure 2

Interactions of PEG/Cor Nps with PC-12 cells. (a) Confocal laser scanning microscope images of PC-12 cells treated with PEG/Cor Nps. (b) The dose-dependent and time-dependent viability and inhibition rate of PC-12 cells in response to PEG/Cor Nps. (c) Confocal layer scanning microscope images of PC-12 cells.

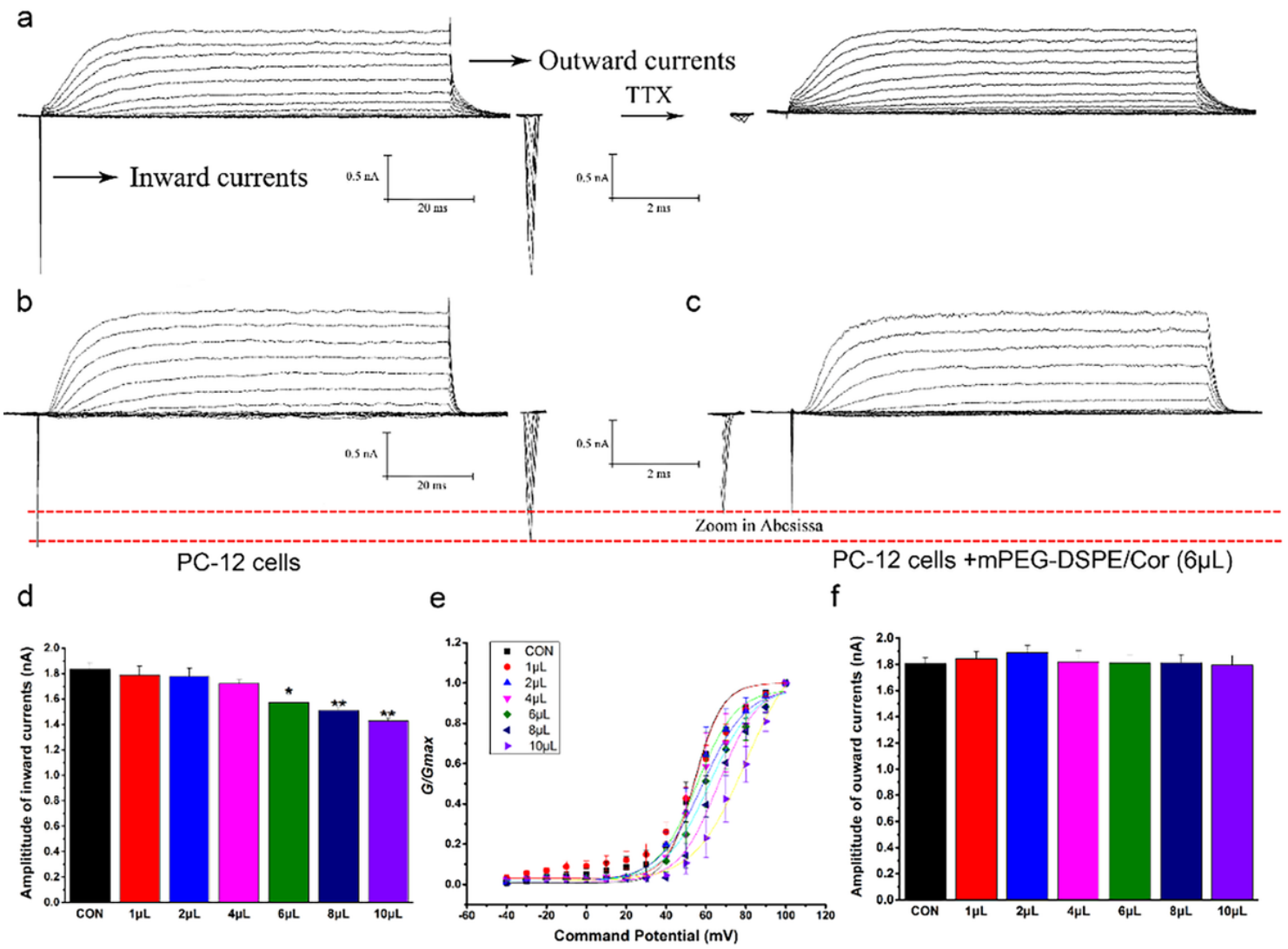

Figure 3

Dose-dependent effects of PEG/Cor Nps on inhibiting voltage-gated Na^+channels activation. (a) Standard ion channel of PC-12 cells and inhibition of sodium ion channels by TTX. (b) Current traces of PC-12 cells. (c) Current traces of PC-12 cells treated with PEG/Cor Nps. Compared with the control group (PC-12 cells), the addition of PEG/Cor Nps did not change the outward current but inhibit the inward current. (d) Inward current amplitude after PEG/Cor Nps treatment. The inward currents were decreased with the increasing of PEG/Cor Nps. (e) Steady-state kinetics of inward currents. The results showed the dose-dependent effects of PEG/Cor Nps on inhibiting inward currents. (f) Outward current amplitude after PEG/Cor Nps treatment.

Figure 4

Time-dependent effects of PEG/Cor complexes on inhibiting voltage-gated Na^+ activation. (a) Current traces of PC-12 cells. (b) Current traces of PC-12 cells treated with PEG/Cor complexes for 10 min. Compared with PC-12 cells, inward current were decreased after co-cultured with PEG/Cor complexes for 10 min. (c) Inward current amplitude after PEG/Cor complexes treatment.The results showed the time-dependent effects of PEG/Cor complexes on inhibiting inward currents. (d)Steady-state kinetics of inward currents.

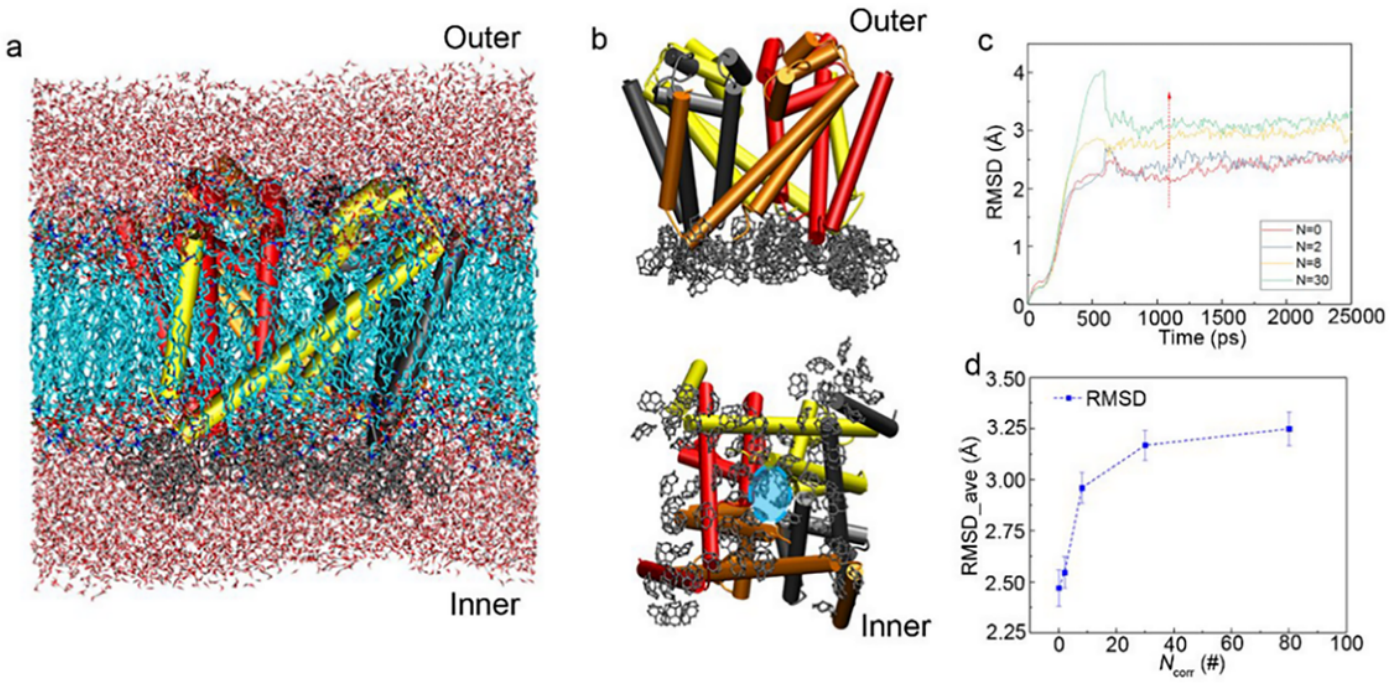

Figure 5

(a) The illustration of the atomic structure of the protein and cell membrane, where the red and white color represents the water molecules, cyan color represents the carbon atoms, and cartoon cylinder represents the structure of the sodium protein. (b) the equilibrated structure of protein and corannulene molecules. (c) The RMSD of protein as a function of the simulation time at a different number of corannulene molecules placed in the system (N =0, 2, 8, and 30). (d) The average RMSD (RMSD_ave) against the number of Cor molecules in the system.

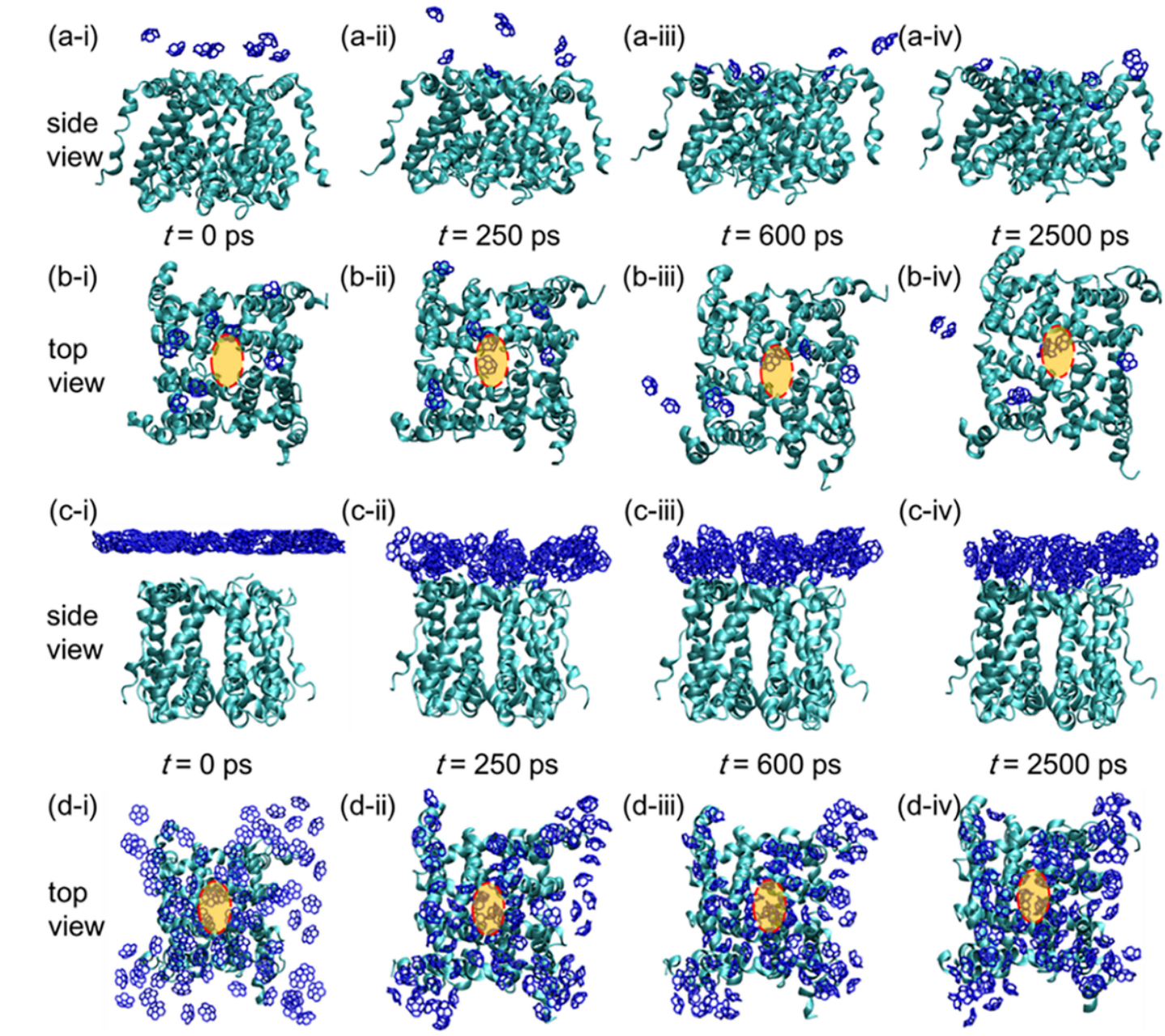

Figure 6

The side and top view of the configuration of Cor and sodium protein at different times, when the number of molecule N = 8 and 80, respectively. (a-b) are for N = 8, while (c-d) are for N =80. In the plots, the water and lipid bilayer membrane is not shown.

Figure 7

(a) The distribution of orientation angle (θ) of Cor against the angle ranging from 0 to 180° for different concentration of Cor in the system. The insert plot represents the definition of the angle, where nz is the z-

direction and *n*c is the vector from bottom to a rim of “molecular bowl”. There are two different configurations: one is “rim-to-protein” state ($\theta > 90°$), indicating that the rim of “molecular bowl” is toward to the protein; the other one is “bottom-to-protein” state ($\theta < 90°$), indicating that the bottom is toward to the protein. (b) The time evolution of orientation angle for different concentration., where two molecules are considering for each concentration as an example.

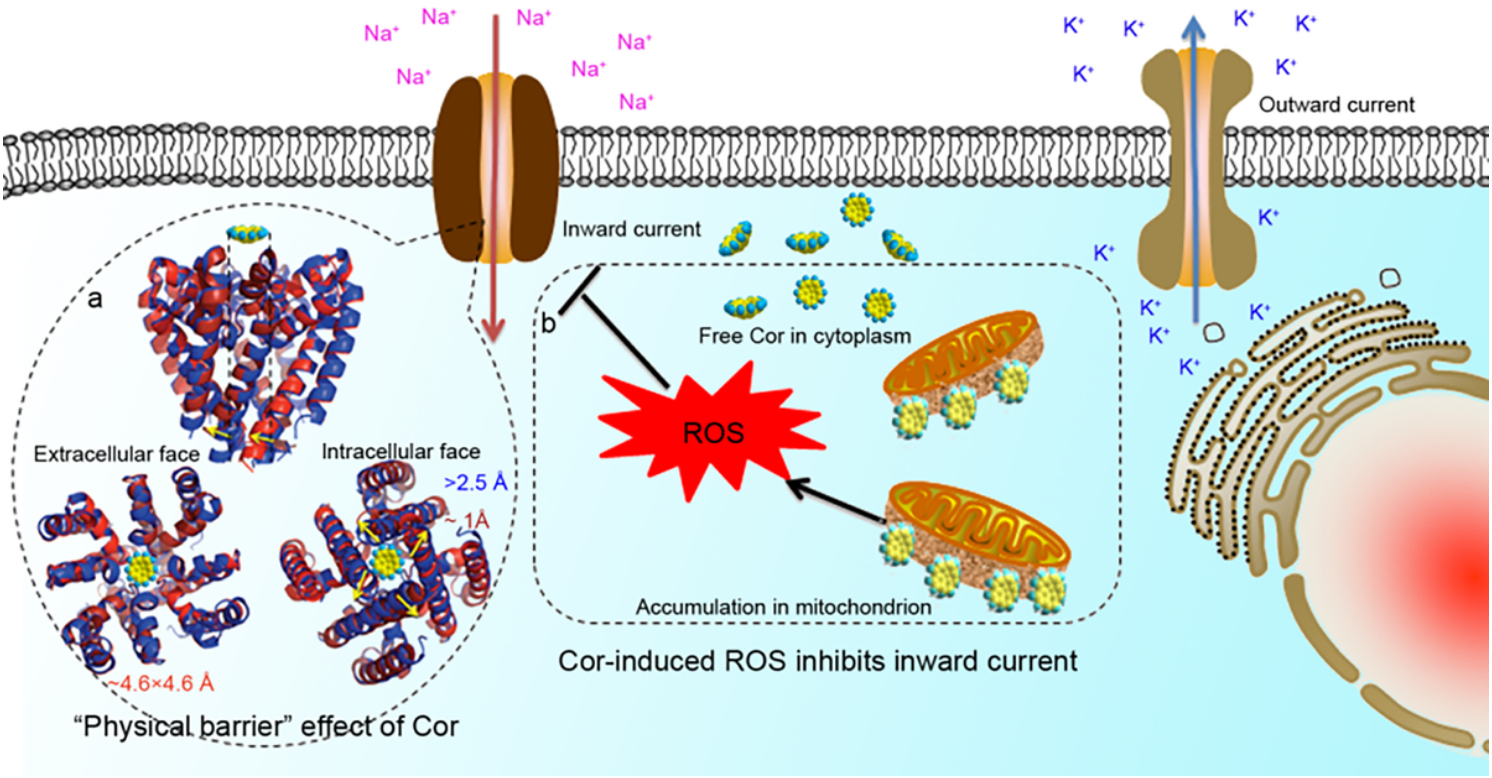

Figure 8

Potential mechanisms of Cor inhibiting voltage-gated Na^+ channel. (a) Cor block voltage-gated Na^+ channel through a pore occlusion mechanisms. (b) Cor-induced production of ROS inhibits voltage-gated Na^+ channel activation.

Supplementary Files

This is a list of supplementary files associated with this preprint. Click to download.

- ManuscriptSI.docx